



UNIVERSITY OF LEEDS

This is a repository copy of *Adaptive Patient-Cooperative Control of a Compliant Ankle Rehabilitation Robot (CARR) with Enhanced Training Safety*.

White Rose Research Online URL for this paper:  
<http://eprints.whiterose.ac.uk/124917/>

Version: Accepted Version

---

**Article:**

Zhang, M, Xie, SQ, Li, X et al. (4 more authors) (2018) Adaptive Patient-Cooperative Control of a Compliant Ankle Rehabilitation Robot (CARR) with Enhanced Training Safety. IEEE Transactions on Industrial Electronics, 65 (2). pp. 1398-1407. ISSN 0278-0046

<https://doi.org/10.1109/TIE.2017.2733425>

---

© 2017, IEEE. This is an author produced version of a paper published in IEEE Transactions on Industrial Electronics. Personal use of this material is permitted. Permission from IEEE must be obtained for all other users, including reprinting/republishing this material for advertising or promotional purposes, creating new collective works for resale or redistribution to servers or lists, or reuse of any copyrighted components of this work in other works. Uploaded in accordance with the publisher's self-archiving policy.

**Reuse**

Items deposited in White Rose Research Online are protected by copyright, with all rights reserved unless indicated otherwise. They may be downloaded and/or printed for private study, or other acts as permitted by national copyright laws. The publisher or other rights holders may allow further reproduction and re-use of the full text version. This is indicated by the licence information on the White Rose Research Online record for the item.

**Takedown**

If you consider content in White Rose Research Online to be in breach of UK law, please notify us by emailing [eprints@whiterose.ac.uk](mailto:eprints@whiterose.ac.uk) including the URL of the record and the reason for the withdrawal request.



[eprints@whiterose.ac.uk](mailto:eprints@whiterose.ac.uk)  
<https://eprints.whiterose.ac.uk/>

# Adaptive Patient-Cooperative Control of a Compliant Ankle Rehabilitation Robot (CARR) with Enhanced Training Safety

Mingming Zhang, Member, IEEE, Sheng Q. Xie, Senior Member, IEEE, Xiaolong Li, Guoli Zhu, Wei Meng, Xiaolin Huang, and Allan Veale

**Abstract**—This paper proposes a new adaptive patient-cooperative control strategy for improving the effectiveness and safety of robot-assisted ankle rehabilitation. This control strategy has been developed and implemented on a compliant ankle rehabilitation robot (CARR). The CARR is actuated by four Festo Fluidic muscles (FFMs) located to the calf in parallel, has three rotational degrees of freedom (DOFs). The control scheme consists of a position controller implemented in joint space and a high-level admittance controller in task space. The admittance controller adaptively modifies the predefined trajectory based on real-time ankle measurement, which enhances the training safety of the robot. Experiments were carried out using different modes to validate the proposed control strategy on the CARR. Three training modes include 1) a passive mode using a joint-space position controller, 2) a patient-robot cooperative mode using a fixed-parameter admittance controller, and 3) a cooperative mode using a variable-parameter admittance controller. Results demonstrate satisfactory trajectory tracking accuracy, even when externally disturbed, with a maximum normalized root mean square deviation (NRMSE) less than 5.4%. These experimental findings suggest the potential of this new patient-cooperative control strategy as a safe and engaging control solution for rehabilitation robots.

**Index Terms**—Adaptive, patient-cooperative, admittance controller, ankle rehabilitation, robot, safety.

Manuscript received June 29, 2016; revised May 09, 2017; accepted July 13, 2017. This work was supported in part by the University of Auckland.

M. Zhang and X. Li are with Tongji Zhejiang College, Jiaying, China. M. Zhang is also with the Department of Mechanical Engineering at the University of Auckland, New Zealand (e-mail: [mzha130@aucklanduni.ac.nz](mailto:mzha130@aucklanduni.ac.nz); [xlionglee@tongji.edu.cn](mailto:xlionglee@tongji.edu.cn)).

S. Q. Xie is with the School of Electronic and Electrical Engineering at University of Leeds, Leeds, UK (corresponding author to e-mail: [S.Q.Xie@leeds.ac.uk](mailto:S.Q.Xie@leeds.ac.uk)).

G. Zhu and X. Huang are with the School of Mechanical Science & Engineering and Tongji Medical College, respectively, at Huazhong University of Science and Technology, Wuhan, China (e-mail: [glzhu@mail.hust.edu.cn](mailto:glzhu@mail.hust.edu.cn); [xiaolin2006@126.com](mailto:xiaolin2006@126.com)).

W. Meng is with the School of Information Engineering, Wuhan University of Technology, Wuhan, China (email: [wmen386@aucklanduni.ac.nz](mailto:wmen386@aucklanduni.ac.nz)).

A. Veale is with the Department of Mechanical Engineering at the University of Auckland, New Zealand (email: [avea007@aucklanduni.ac.nz](mailto:avea007@aucklanduni.ac.nz)).

## I. INTRODUCTION

ROBOT-assisted ankle rehabilitation solutions, as therapeutic adjuncts to facilitate clinical practice, have been actively researched in the past few decades. Two types of ankle robots are wearable devices such as the MIT Anklebot [1] and the bio-inspired soft ankle robot [2], and platform ones [3-7]. Zhang, et al. [8] systematically reviewed a variety of ankle rehabilitation devices and demonstrated that robot-assisted rehabilitation techniques are effective in reducing ankle impairments. They also demonstrated that wearable robots are more suitable for gait training, while platform ones are better suited for ankle exercises only.

Platform robots can have a single degree of freedom (DOF) or multiple DOFs. The single-DOF one is generally actuated by a rotating motor [3], while multi-DOF ones are usually based on parallel mechanisms [4-7]. Further, the parallel robot whose actuators locate below its end effector has a misaligned rotation center with the ankle joint [6, 7]. This requires synergic movement of the shinbone from the patient for ankle training, which causes discomfort to patients and even hurts the ankle joint. By contrast, patients can keep their shanks stationary on leg holders on devices with actuators installed above their end effectors [4, 5]. From this point of view, parallel robots actuated from above are more suitable for ankle rehabilitation due to better alignment of the robot and the ankle joint.

Many rehabilitation strategies have been implemented on existing ankle robots [8]. Zhang, et al. [3] developed an intelligent ankle stretching device. This device only allows training along ankle dorsiflexion/plantarflexion (DP) although its effectiveness has been verified on children with cerebral palsy [9] and stroke patients [10]. The Rutgers Ankle was proposed based on a six-DOF Stewart-Gough platform [7]. It has been able to conduct both passive and active rehabilitation exercises by integrating real-time assessment, virtual-reality games, and tele-rehabilitation techniques [11]. Saglia, et al. [6] constructed a parallel ankle rehabilitation robot with two DOFs (ankle DP and inversion/eversion (IE)). While an interaction control algorithm has been implemented through a position controller for passive training and an admittance controller for active training [12], it does not consider adaptive adaptation of the control parameters. These robots suffer from limited DOFs

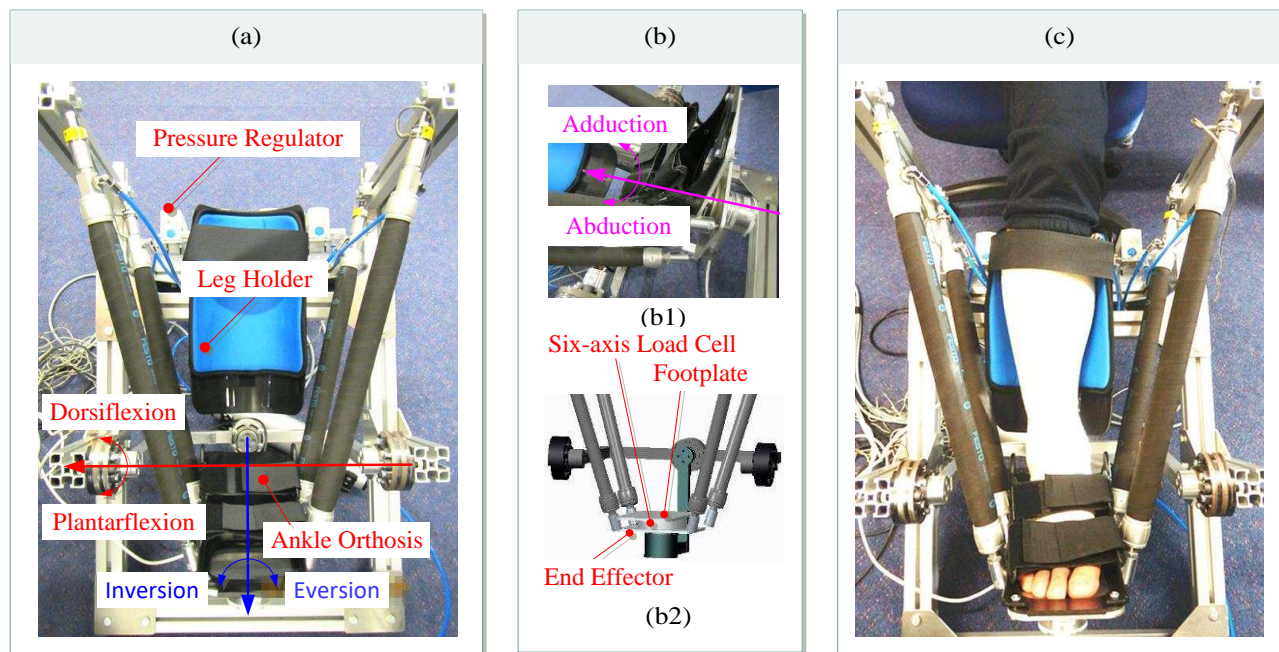


Fig. 1. An ankle rehabilitation robot with three rotational DOFs. (a) The CARR, the red and blue arrow lines represent the axes of ankle DP and IE; (b1) The end effector with a six-axis load cell for the measurement of patient-robot interaction forces and torques, the pink arrow line represents the axis of ankle AA; (b2) The mechanical design to show the installation of the six-axis load cell; and (c) The CARR in use on a patient.

or misaligned rotation center. Jamwal, et al. [4] developed a parallel ankle rehabilitation robot using four pneumatic artificial muscles. This robot has an aligned rotation center with the ankle joint. While satisfactory trajectory tracking was achieved using an adaptive fuzzy-logic position controller, the adaptation law was only for the length control of the muscle rather than real-time patient-robot interaction. In brief, this control method does not allow active training on this robot.

To overcome the abovementioned limitations of existing ankle rehabilitation robots, our group recently developed a compliant ankle rehabilitation robot (CARR). This robot has advantages including aligned rotation center, three DOFs, compliant actuation, and real-time measurement of patient-robot interaction. These features make the CARR have great potential for ankle rehabilitation. However, an interactive controller that can maximize the performance of the CARR has not been designed and validated. Such a training strategy can improve the training safety and therapeutic outcome by introducing a certain amount of robot compliance, and adapting robot behavior to patients' ankle abilities.

## II. COMPLIANT ANKLE REHABILITATION ROBOT (CARR)

The CARR, as a parallel mechanism, consists of a fixed platform and a moving platform, of which the moving one is a

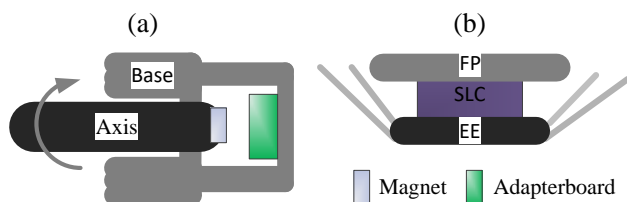


Fig. 2. Sensors installation in the CARR: (a) the magnetic rotary encoder for measuring the angular position of a single axis; (b) the six-axis load cell (SLC) for detecting patient-robot interaction. FP: Footplate, EE: End effector.

three-link serial manipulator. It is actuated by four Festo Fluidic muscles (FFMs) (DMSP-20-400N) for three rotational DOFs. Ankle DP and IE are labeled in Fig.1 (a), and ankle adduction/abduction (AA) is labeled in Fig.1 (b1). These three motions are denoted by red, blue, and pink lines, respectively. The arrow line represents the rotation axis.

Four proportional pressure regulators (Festo VPPM-6L-L-1-G18-0L6H) are used for pressure control of four FFMs. For the sensing function of the CARR, three magnetic rotary encoders (AMS AS5048A) are used about each rotation axis for measuring angular positions of the end effector, a six-axis load cell (SRI M3715C) is located between the footplate and the end effector for measuring patient-robot interaction, as shown in Fig. 1(b2) and Fig. 2. It is hypothesized that there is no relative motion between the footplate and the patient's foot during the training, thus the measured position of the end effector equals that of the involved foot. Fig. 1(c) presents the use of the CARR on a subject. These electronic components communicate with the embedded controller (NI Compact RIO 9022) through three modules (NI 9401, NI 9205 and NI 9263) for digital input/output, analog input, and analog output, respectively.

## III. ADAPTIVE PATIENT-COOPERATIVE CONTROL

A new patient-cooperative control strategy on the CARR based on real-time patient-robot interaction is shown in Fig. 3. It consists of a joint-space position controller (low-level) and a task-space admittance controller (high-level).

### A. Joint-Space Position Controller

A position controller serves as a low-level controller for patient-cooperative robotic training. The trajectory tracking of the CARR could be achieved by controlling individual FFM length in joint space. As in Fig. 3, the desired individual FFM length is calculated by inverse kinematics based on predefined

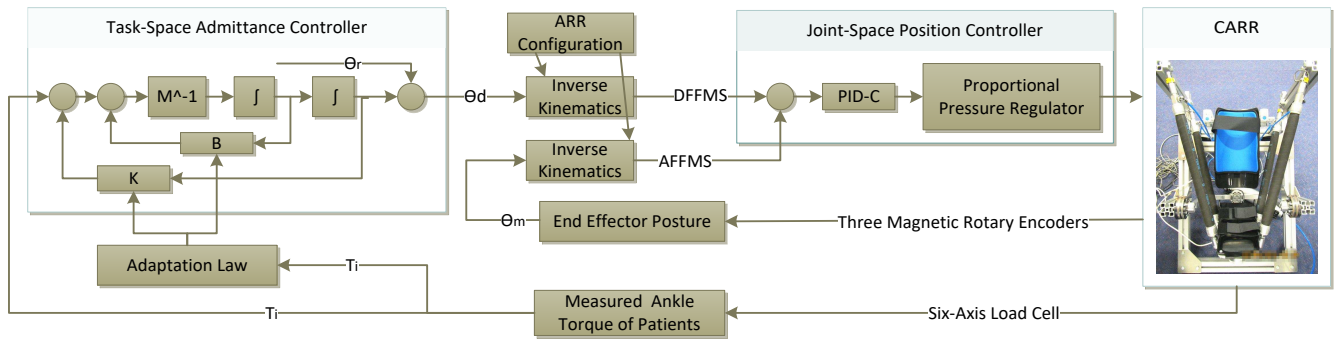


Fig. 3. An adaptive patient-cooperative control strategy implemented on the CARR with a position controller in joint space and an admittance controller in task space. DFFML: Desired Festo Fluidic muscle length; MFFML: Measured Festo Fluidic muscle strain; PID-C: Proportional-integral-derivative controller; Adaptation law refers to Fig. 3 and (16-17); and ankle force and torque are calculated using (8);  $\theta_r$  is the reference position, and the position tracking error is denoted by  $\theta_e$ ,  $\theta_e = \theta_d - \theta_m$ , of which  $\theta_d$  represents the desired position of the end effector while  $\theta_m$  is the measured position;  $T_i$  represents the interaction torque.

trajectories, while, as the feedback to the proportional-integral-derivative (PID) controller, the actual individual FFM length is obtained based on measured posture of the CARR. This controller outputs four individual pressure values that directly go to VPPMs for actuating the four FFMs.

More specifically, the desired trajectory is denoted as  $\theta_d(t)$  in (1). The measured trajectory is obtained from three magnetic rotary encoders and denoted as  $\theta_m(t)$  in (1). The subscripts DP, IE and AA represent ankle dorsiflexion/plantarflexion, inversion/eversion, and adduction/abduction, respectively. Individual FFM length is calculated using (2) based on inverse kinematics, where  $l_{4 \times 1}^d(t)$  and  $l_{4 \times 1}^m(t)$  respectively represent desired and measured FFM lengths,  $\mu$  is a coefficient that relates the FFM length to the link length depending on the CARR configuration,  $\mathcal{N}_{4 \times 3}$  relates the link length to the posture of the robot. Lastly, the error  $e_{4 \times 1}(t)$  shown in (3) is input to the PID controller, and the individual desired FFM pressure can be calculated according to (4) with well-tuned  $K_p$ ,  $K_i$ , and  $K_d$ .

$$\begin{cases} \theta_d(t) = [\theta_{DP}^d(t) & \theta_{IE}^d(t) & \theta_{AA}^d(t)]^T \\ \theta_m(t) = [\theta_{DP}^m(t) & \theta_{IE}^m(t) & \theta_{AA}^m(t)]^T \end{cases} \quad (1)$$

$$\begin{cases} l_{4 \times 1}^d(t) = \mu \mathcal{N}_{4 \times 3} \theta_d(t) \\ l_{4 \times 1}^m(t) = \mu \mathcal{N}_{4 \times 3} \theta_m(t) \end{cases} \quad (2)$$

$$e_{4 \times 1}(t) = l_{4 \times 1}^d(t) - l_{4 \times 1}^m(t) \quad (3)$$

$$p_{4 \times 1}(t) = K_p e_{4 \times 1}(t) + K_i \int_0^t e_{4 \times 1}(t) dt + K_d \frac{de_{4 \times 1}(t)}{dt} \quad (4)$$

## B. Task-Space Admittance Controller

The interaction tasks cannot be handled by pure motion control that rejects forces exerted by patients as disturbances. Impedance and admittance control schemes are usually considered as the basis of interactive robotic training. The impedance controller takes a displacement as input and reacts with a force. To apply on the CARR, the impedance control law can be considered as (5). The desired driven torque is calculated based on (6) and (7). An analytic-iterative technique proposed by Taghirad and Bedoustani [13] can be used to distribute the desired robot torque to individual desired FFM force. However, it is challenging to be implemented on the CARR due to high requirement of the robotic assembly

precision. Engagements from patients also induce sudden FFM force changes, which can make the system unstable.

$$T_i(t) - T_i^d(t) = M(\ddot{\theta}_d(t) - \ddot{\theta}_m(t)) + B(\dot{\theta}_d(t) - \dot{\theta}_m(t)) + K(\theta_d(t) - \theta_m(t)) \quad (5)$$

$$T_r(t) - T_i(t) = M\ddot{\theta}_m(t) + C\dot{\theta}_m(t) + C_f\theta_m(t) + G \quad (6)$$

$$T_r(t) = 2T_i(t) - B(\dot{\theta}_d(t) - \dot{\theta}_m(t)) - K(\theta_d(t) - \theta_m(t)) + C\dot{\theta}_m(t) + C_f\theta_m(t) + G \quad (7)$$

In admittance control mode, by contrast, the robot assumes the behavior of admittance and its movements are determined by the external force from patients. Under this mode, the CARR deviates from the reference trajectory in the presence of patient-robot interaction but is otherwise following the reference trajectory. Thus, an adaptive admittance controller is developed on the CARR for patient-cooperative training. The admittance control law is proposed in (8), where  $\theta_r(t)$  and  $\theta_d(t)$  represent the reference trajectory and the recalculated desired trajectory, respectively, and  $T_i(t)$  is the patient-robot interaction torque,  $B$  and  $K$  respectively represent the damping and stiffness coefficients. The end effector of the CARR is a three-link serial manipulator whose inertia tensor  $M$  is calculated based on (9).

The integration of the feed forward measured patient-robot interaction torque, in Fig.3, allows for a variable admittance controller for adaptive training. Patient-robot interaction forces and torques are calculated using readings of the six-axis load cell in (10) [14], where  $F$  and  $T$  represent forces and torques, the script  $a$  and  $slc$  represent the ankle joint and the six-axis load cell,  ${}_{slc}^a R$  is a  $3 \times 3$  rotation matrix from  $a$  to  $slc$ ,  $P_{slc}^a \times {}_{slc}^a R$  is a  $3 \times 3$  skew matrix from  $a$  to  $slc$ , and  $P_{slc}^a$  is defined in (11).

$$T_i(t) = M(\ddot{\theta}_d(t) - \ddot{\theta}_r(t)) + B(\dot{\theta}_d(t) - \dot{\theta}_r(t)) + K(\theta_d(t) - \theta_r(t)) \quad (8)$$

$$M(\theta_{DP}, \theta_{IE}, \theta_{AA}) = \sum_{i=1}^3 M_i = \sum_{i=1}^3 R_i I_i R_i^T \quad (9)$$

$$\begin{bmatrix} F_{3 \times 1}^a \\ T_{3 \times 1}^a \end{bmatrix} = \begin{pmatrix} {}_{slc}^a R & 0_{3 \times 3} \\ P_{slc}^a \times {}_{slc}^a R & {}_{slc}^a R \end{pmatrix} \begin{bmatrix} F_{3 \times 1}^{slc} \\ T_{3 \times 1}^{slc} \end{bmatrix} \quad (10)$$

$$P_{slc}^a = \begin{bmatrix} 0 & -p_z & p_y \\ p_z & 0 & -p_x \\ -p_y & p_x & 0 \end{bmatrix} \quad (11)$$

To ensure the safety of the proposed patient-cooperative control strategy, the bounded input and bounded output (BIBO) stability of the admittance controller is conducted. Equation (8) can be rewritten in (12), and (13) is further obtained, where  $T_d(t) = M(t)\ddot{\theta}_d(t) + B(t)\dot{\theta}_d(t) + K(t)\theta_d(t)$ . System transfer function (15) is obtained through Laplace transformation (14). Based on (16), this system is BIBO stable, since all eigenvalues are in the open left half plane with  $B > 0$  and  $M > 0$ .

$$\begin{aligned} M(t)\ddot{\theta}_d(t) + B(t)\dot{\theta}_d(t) + K(t)\theta_d(t) \\ = T_i(t) + M(t)\ddot{\theta}_r(t) \\ + B(t)\dot{\theta}_r(t) + K(t)\theta_r(t) \end{aligned} \quad (12)$$

$$T_i(t) = T_d(t) - M(t)\ddot{\theta}_r(t) - B(t)\dot{\theta}_r(t) - K(t)\theta_r(t) \quad (13)$$

$$T_i(s) = -[M(s)s^2 + Bs + K]X(s) \quad (14)$$

$$\frac{X(s)}{T_i(s)} = \frac{-1}{M(s)s^2 + B(s)s + K(s)} \quad (15)$$

$$s = \frac{-B \pm \sqrt{B^2 - 4MK}}{2M} \quad (16)$$

### C. Adaptation Law

Ankle stiffness varies over its range of motion (ROM) during robot-assisted rehabilitation training. To guarantee training safety, it is important for the robot to provide assistive torque with adjustable compliance. While the CARR can be programmed to carry out both passive and interactive training, an adaptive interaction control scheme is required for enhanced rehabilitation efficacy and training safety.

A new adaptation law is proposed in this study to tune the admittance parameters of the CARR based on real-time ankle posture and interaction torque. Specifically, the parameters  $B$  and  $K$  are adapted by rules (17) and (18), where  $B_0$  and  $K_0$  are base values,  $a_1$ ,  $a_2$ , and  $a_3$  are weighting coefficients that adjust the influences of the angular position,  $b_1$ ,  $b_2$ , and  $b_3$  are used to adjust the influence of the interaction torque.

$$B = \begin{cases} B_{11}, & \text{if } B < B_{11} \\ B_0 \frac{1}{a_1 e^{|a_2 \theta|}} \left| a_3 \frac{T_{\text{modeling}}}{T_{\text{measured}}} \right|, & \text{if } B_{11} \leq B \leq B_{12} \\ B_{12}, & \text{if } B > B_{12} \end{cases} \quad (17)$$

$$K = \begin{cases} K_{11}, & \text{if } K < K_{11} \\ K_0 \frac{1}{b_1 e^{|b_2 \theta|}} \left| b_3 \frac{T_{\text{modeling}}}{T_{\text{measured}}} \right|, & \text{if } K_{11} \leq K \leq K_{12} \\ K_{12}, & \text{if } K > K_{12} \end{cases} \quad (18)$$

To reduce the effect of the angular dependency of passive ankle torque, the interaction torque is normalized by a model-based predicted passive torque. The involvement of the subject-specific passive ankle torque is expected to minimize the effects of different sizes of participants. Stiffness and damping parameters are bounded by saturation functions to

guarantee the stability of the control system. The proposed adaptation law reduces the robot stiffness and damping as the robot angular displacement and interaction torque increase. This ensures that the patient is able to safely backdrive the CARR even when the foot is took into an uncomfortable position, and so prevents a large and potentially harmful contact force and torque.

## IV. SIMULATION

To verify the feasibility of the admittance controller with the adaptation law, a MATLAB simulation was conducted. It is shown in Fig. 4 that the patient-robot interaction torque deviates the robot trajectory from the reference one. This can increase motivation and active participation of patients as his/her movement intention and active effort are reflected by the adaptation of the robot trajectory. Adaptation of the training trajectory is also influenced by damping and stiffness parameters, which enables the robot to provide assistance with adjustable compliance. When the ankle is highly extended or exerts a large interaction torque, the robot behaves with a high compliance for training safety. In this situation, the movement of the robot can be adjusted by patients, and thus the trajectory deviation can be prominent. On the other hand, the trajectory deviation is slight when the robot is running in a more passive way with a low robot compliance. Meanwhile, constraints on the robot ROM and compliance are enforced by using saturation functions to prevent endangerment to patient safety. It should be noted that this algorithm suits for any movement, not limited to the three DOFs of the CARR.

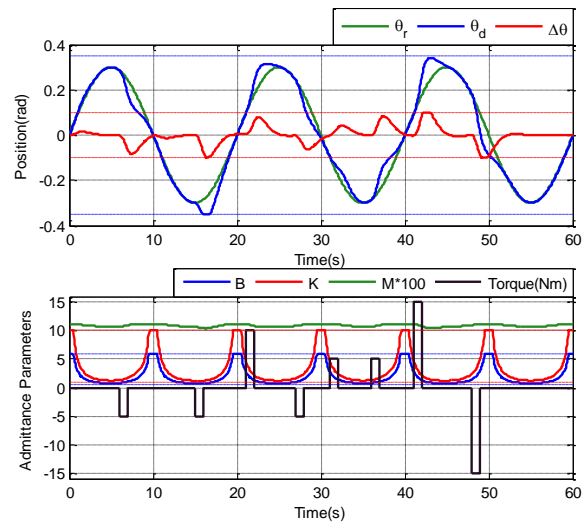


Fig. 4. Simulation of the admittance controller with an adaptive adaptation law. The recalculated desired trajectory  $\theta_d$  is determined by the reference trajectory  $\theta_r$  and the deviated value  $\Delta\theta$ , which is calculated by (8). Here  $-0.1 \leq \Delta\theta \leq 0.1$ ,  $-0.35 \leq \theta_d \leq 0.35$ . The saturation function is denoted by the red and blue dotted lines respectively. The damping  $B$  and stiffness  $K$  are determined by the robot's angular position, interaction torque, and the modeled ankle torque. They are adapted using (17) and (18). Here,  $0.6 \leq B \leq 6$ ,  $1 \leq K \leq 10$ . The saturation function is denoted by the blue and red dotted lines respectively.  $M$  is the inertial parameter calculated of the CARR. To get a clear view of its changes,  $M$  is multiplied by 100 times.

In Fig. 4, the cyan curve represents the reference trajectory, the desired trajectory is adaptively deviated from the reference

one based on real-time patient-robot interaction, plot in blue, the red line shows the deviation of these two trajectories. Fig. 4 also shows the values of B, K and M and the interaction torque, of which B and K are adaptively tuned by (17) and (18).

## V. EXPERIMENTAL RESULTS

A musculoskeletally injured subject (male, 29 years) with ankle sprain, and a neurologically injured subject (male, 68 years) with drop foot participated in this study. The sprained ankle was due to jumping and rolling during basketball and diagnosed as limited ROM and torn ligaments. The drop foot was caused by stroke. Both gave written consent to participate in the trial according to ethics approval obtained from the University of Auckland, Human Participants Ethics Committee (011904).

TABLE I

THREE TRAININGS APPLIED TO THE SUBJECT WITH ANKLE SPRAIN

Training Modes	X (rad)		Y (rad)	
	Dorsiflexion	Plantarflexion	Inversion	Eversion
PT	0.3	0.3	0.1	0.1
PCT with FA	0.2	0.2	0	0
PCT with VA	0.2	0.2	0	0

PT: Passive training, PCT: Patient-cooperative training; FA: Fixed admittance; VA: Variable admittance.

### A. Experimental Protocol

Before the training, a preliminary assessment was conducted to check the appropriate ROMs of the drop foot and the sprained ankle by a doctor. Each of them was instructed to sit on a height-adjustable chair with the shank free on the leg holder, as shown in Fig. 1(c). Their feet were strapped into the ankle orthosis during the training. The patient with drop foot has very limited active ankle ROM, thus only passive stretching along ankle DP was conducted based on the doctor's suggestion. The subject with ankle sprain can conduct both passive and active training along ankle DP and IE, with very limited active ROM of ankle IE. Although the CARR was designed with three DOFs, only training along DP and IE was conducted. The doctor did not suggest any training along ankle AA.

The training trajectory prescribed to the drop foot is a sine wave with the frequency of 0.02 Hz. Its amplitude was initially set at 0.1 rad, and then gradually increased until a feeling of joint tightness. The subject was verbally encouraged to relax his foot to minimize the effects by active contributions. The whole process lasted 15 minutes with 18 cycles. On the sprained ankle, three types of trainings were conducted, as summarized in Table I. They are 1) passive mode using only position control in joint space, 2) patient-cooperative training using a fixed- admittance controller, and 3) patient-cooperative training using a variable-admittance controller. The passive mode followed a mixed trajectory of ankle DP and IE, while the patient-cooperative training was conducted along only ankle DP. These trajectories were set to operate three cycles of sine wave at 0.05 Hz. The parameters of the admittance controller were determined based on trial and error. Optimization

techniques are required for optimal parameter selection. In this study, ankle DP, IE and AA are respectively denoted as X, Y and Z to simplify the description.

### B. Model-Based Passive Ankle Torque

The estimated passive ankle torque can be obtained from a computational ankle model that has three rotational DOFs with 12 muscles and seven ligaments [15]. The modeling results on the participant with ankle sprain are presented in Fig. 5. To facilitate its use with the variable-admittance controller in real-time, an approximation equation (19) is fitted to the numerical model to estimate passive ankle torque, where  $p_1 = 5.1992$ ,  $p_2 = 1.6238$ ,  $p_3 = 9.7792$ , and  $p_4 = 0.2927$ .

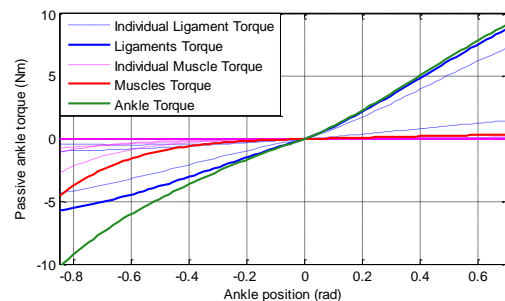


Fig. 5. Model-based passive joint torque of the sprained ankle.

$$T_{\text{modeling}} = p_1 \theta_m(t)^3 + p_2 \theta_m(t)^2 + p_3 \theta_m(t) + p_4 \quad (19)$$

### C. Position Control

Experimental results on the drop foot are presented in Fig. 6. In the first 100 seconds, the training trajectory has an amplitude of 0.1 rad. Based on the patient's feedback, the robot ROM was gradually increased until a feeling of joint tightness. During the period of 100<sup>th</sup> to 200<sup>th</sup> seconds, the amplitude of the trajectory was increased to 0.15 rad. It was further increased to 0.2 rad after the 200<sup>th</sup> second, when the patient felt slightly tight at his ankle joint. The robot kept this trajectory during the period of 200<sup>th</sup> to 725<sup>th</sup> seconds. As the patient requested, the amplitude of the training trajectory was finally adjusted to 0.25 rad when the patient felt obvious ankle stretching. The statistical results of the trajectory tracking accuracy are encouraging with the root mean square deviation (RMSD) value being 0.0408 rad and the normalized root mean square deviation (NRMSD) value being 8.16%.

Experimental results on the sprained ankle are presented in Fig. 7 and 8. The trajectory tracking in task space is shown in Fig. 7, and individual muscle length tracking in joint space is plot in Fig. 8. The trajectory tracking performance is satisfactory in both task space and joint space, with all NRMSD values in task space less than 5.4% and those in joint space no greater than 4.71%, as summarized in Table II at the end of Section V.

### D. Patient-Cooperative Training

Patient-cooperative training was first evaluated using the fixed-admittance controller on the sprained ankle. Parameters B and M were both set at a constant value of 0.03. Experimental

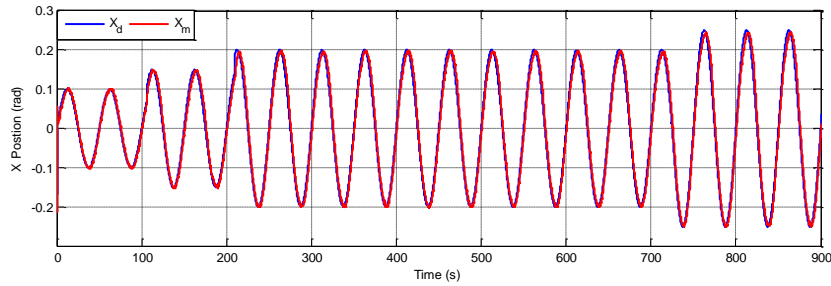


Fig. 6. Trajectory tracking responses during passive training on the drop foot.

results are presented in Fig. 9, where satisfactory performance is achieved for the position tracking of the robot and real-time interaction torque is recorded. Statistical results of the trajectory tracking about X are summarized in Table II, with the NRMSD value being 3.26%. It is shown in Fig. 9 that by using the admittance controller the recalculated desired trajectory deviates from the reference path in accordance with the interaction torque  $T_x$ . For instance, the recalculated trajectory deviates from its reference path to move towards plantarflexion when  $T_x$  is in negative direction during 0-10 seconds. The robot deviates and moves towards dorsiflexion during 12-18 seconds when positive interaction torque is applied. The robot ROM is bounded for preventing ankle hyperflexion or hyperextension, which is reflected during 54 to 57 seconds.

The patient-cooperative training was then evaluated using the variable admittance controller on the sprained ankle, with B and M being adjusted based on (17) and (18). Experimental results are presented in Fig. 10. The real-time adaptive damping and stiffness coefficients are recorded as well as the measured interaction torque. Table II summarizes the statistical results of the trajectory tracking accuracy about X, with the NRMSD value being 3.77%. The robot ROM is bounded between -0.35 and 0.35 rad for training safety when continuous interaction torque exists. The deviated movement for a certain moment is limited between -0.1 and 0.1 rad to prevent sudden changes of the trajectory. The damping and stiffness coefficients remain inside a constrained space between 0.01 and 0.1 to guarantee the system stability.

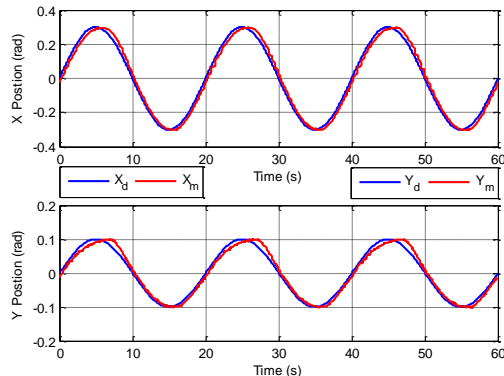


Fig. 7. Trajectory tracking during passive training on the sprained ankle.

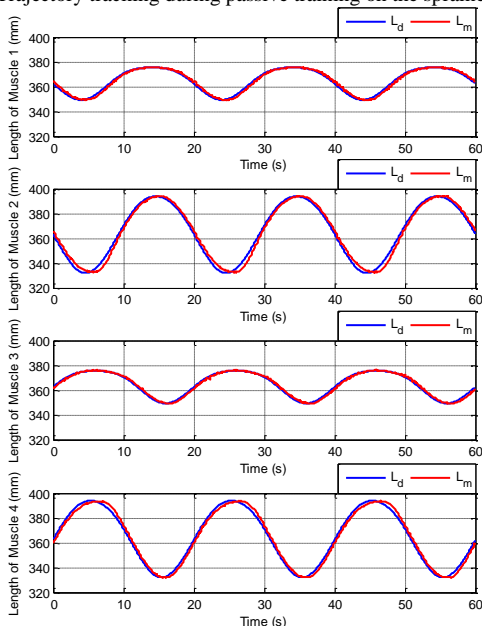


Fig. 8. Muscle length tracking during passive training on the sprained ankle.

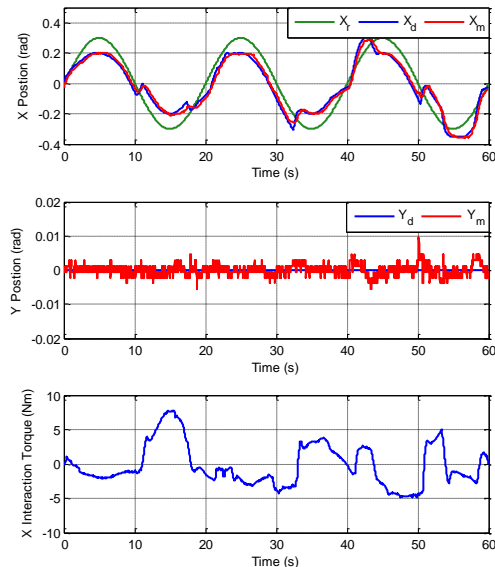


Fig. 9. Trajectory tracking of the patient-cooperative training with fixed admittance.

The passive ankle torque is small when the ankle is close to its neutral position and increases when it goes to its limited position, as shown in Fig. 5. It can be seen from Fig. 10 that the interaction torque depends on both ankle position and patient's active engagement with the robot. The interaction torque tends to be larger for a higher ankle extension, although certain rapid changes exist due to the patient's subjective intention. Parameters B and K increase as the interaction torque decreases while decrease as the interaction torque increases during 15-20 seconds. The adaptation law is also influenced by the modeling torque and the ankle position. For instance, parameters B and K are small during 4-5 seconds when the interaction torque is small, which can be accounted for by large ankle flexion and model predicted torque. This adaptation law allows the robot to

be more compliant in extended ankle position compared to its neutral position. Specifically, it is easier for the patient to change the robot movement with lower B and K values, such as during the periods of 30-35 and 52-57 seconds. In contrast, during the periods of 7-10 and 38-41 seconds, the robot is operating in a more passive mode with high B and K values, limiting backdrivability.

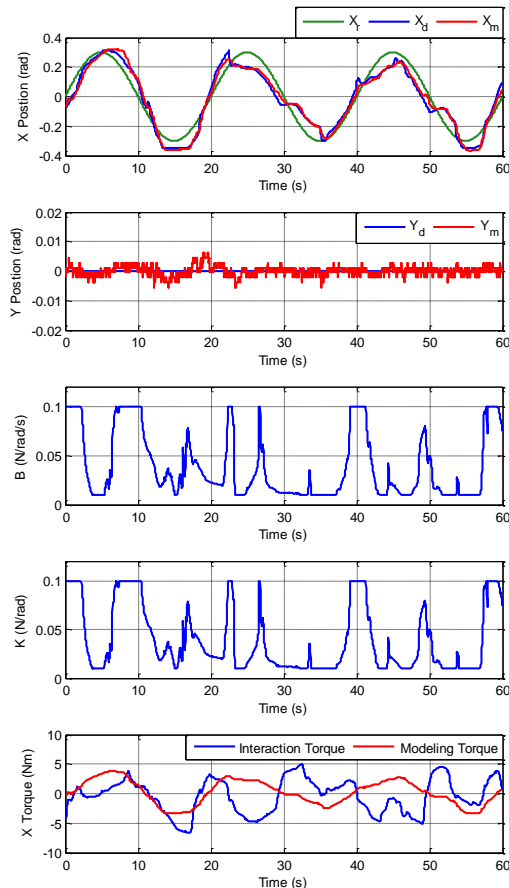


Fig. 10. Trajectory tracking responses of the patient-cooperative training with variable admittance.

As experimental results presented in Fig. 9 and Fig. 10, the patient-cooperative control strategy with fixed admittance or variable admittance has been used in both passive and active training. If a patient does not exert any active torque above the defined threshold, the robot operates in a passive mode to track the predefined trajectory. Otherwise, the robot runs in a patient-cooperative mode under the admittance control strategy. The adaptive patient-cooperative control scheme, however, presents advantages compared to that with fixed admittance based on a fact that the robot should be more compliant with a stiffer joint. For instance, adapting robot compliance according to joint stiffness increases robot backdrivability at ankle limits, thus making patients safer and more comfortable. This realizes the remark of Riener, et al. [16] who suggested that robot-assisted training with real-time assessment will likely make therapy easier, more efficient, and comfortable.

## VI. DISCUSSION AND CONCLUSION

Two typical control schemes of parallel robots are the joint

TABLE II

STATISTICAL RESULTS OF THE CONTROL PERFORMANCE ON THE CARR

		PT	PCT with FA	PCT with VA
X	RMSD (rad)	0.0247	0.0223	0.0251
	NRMSD (%)	4.12	3.26	3.77
Y	RMSD (rad)	0.0107	0.0016	0.0017
	NRMSD (%)	5.36	—	—
ML 1	RMSD (mm)	1.1345	—	—
	NRMSD (%)	4.34	—	—
ML 2	RMSD (mm)	2.9144	—	—
	NRMSD (%)	4.71	—	—
ML 3	RMSD (mm)	0.9861	—	—
	NRMSD (%)	3.77	—	—
ML 4	RMSD (mm)	2.5954	—	—
	NRMSD (%)	4.20	—	—

RMSD: Root mean square deviation; NRMSD: Normalized root mean square deviation; PT: Passive training, PCT: Patient-cooperative training; ML: Muscle length; FA: Fixed admittance; VA: Variable admittance; — represents not applicable.

space controller and the task space controller. The joint space controller, for position control, is to make actual link lengths conform to desired lengths computed from the required position of the manipulator by inverse kinematics [17]. In a similar way, a joint space force controller is also achievable if force distribution can be conducted for a given robotic torque. This method, however, is subject to numerical optimization [13]. In this study, the joint space position controller was selected as the basis of the patient-cooperative control strategy. This is due to the fact that the force distribution of the CARR with minimum energy consumption cannot be obtained in real time.

Adaptive interaction control strategies have been developed in different ways. A common method is based on the trajectory tracking error [18-20]. Lu, et al. [21] developed an adaptive control scheme by incorporating learning control approaches into an exoskeleton to handle periodic uncertainties. The patient's disability level and active engagement have been also considered for more advanced adaptation laws. Hussain, et al. [22] proposed an adaptive impedance controller that adjusts the assistance of a robotic gait orthosis according to the disability level and voluntary participation of human subjects. Jamwal, et al. [23] used a similar control strategy on a parallel ankle robot. While estimation of voluntary participation could result in adaptive robotic assistance, the identification of active joint torque is subject to inverse dynamics and estimation of passive joint torque [24].

Rehabilitation therapists advocated the assistance-as-needed (AAN) control strategy. Recent studies have investigated this novel training scheme to keep a challenging assistance level to avoid slacking. Emken, et al. [25] designed an error-based tracking controller with a forgetting factor for providing assistance only as needed. Wolbrecht, et al. [26] introduced a forgetting factor for adaptive control to decay the robotic assistance when errors in task execution are small. Banala, et al. [27] gradually increased the difficulty level by reducing the robotic assistance and increasing the treadmill speed when patients achieved better tracking performance. These robotic interaction controllers behave like: they create restoring forces

if participants deviate from desired trajectories. Otherwise, if the tracking error is acceptable, the controller will not intervene. In addition, Pérez-Rodríguez, et al. [28] proposed a new AAN control algorithm to provide anticipatory actuation. To tailor the therapy for each patient, Metzger, et al. [29] adapted exercise difficulty based on an assessment-driven selection for hand training. The focus of such adaptation algorithms is that the robot torque varies over time to continuously challenge the patient to exert his/her own effort and thus actively engage in the rehabilitation treatment [26]. However, as each algorithm has its own specific advantages related the platform on which it is implemented, there is no obvious golden standard for online difficulty adaptation of the training.

Back to Figs 9, 10, the patient-cooperative control strategies with fixed admittance or variable admittance both have shown great potentials for clinical applications. However, a quantitative comparison between fixed admittance and variable admittance is lacking, although statistical data are present in Table II. The admittance parameters were determined based on trial and error in this study, and for optimal control performance optimization techniques are required for most appropriate parameters. This will be carried out in future, as well as a direct comparison between fixed admittance and variable admittance on a large sample of participants.

The proposed techniques in this study contribute to enhanced effectiveness and safety of robot-assisted ankle rehabilitation training from four aspects. One is the use of compliant actuators making the training safer and more comfortable. Next, the robot has three rotational DOFs for comprehensive ankle exercises. Third, the parallel mechanism based robot designed with appropriate workspace can ensure the robotic training in a safe range of motion. Last is the development of an adaptive admittance controller. It adaptively modifies the predefined trajectory based on real-time ankle measurement (ankle posture and interaction torque) to ensure training safety by avoiding excessive interaction forces and torques.

While Krebs, et al. [30] suggested that therapy should be tailored to each patient and there is no "one-size-fits-all" control strategy, however, it can be assumed that the proposed patient-cooperative control is a "one-size-fits-most" control scheme. This algorithm allows the CARR to adaptively conduct either passive or cooperative training based on real-time assessment from subject-specific modeling results and built-in sensors. Preliminary findings on a drop foot and a sprained ankle are encouraging, which demonstrates adaptive robust and accurate trajectory tracking and thus establishes its efficacy. To the best of the authors' knowledge, the admittance control on a parallel mechanism with actuators below its end effector has not been reported in literature. The proposed adaptation law for adjusting admittance parameters based on real-time ankle position, interaction torque, and passive ankle torque is also novel.

## REFERENCES

- [1] A. Roy et al., "Robot-aided neurorehabilitation: a novel robot for ankle rehabilitation," *IEEE Transactions on Robotics*, Article vol. 25, no. 3, pp. 569-582, 2009.
- [2] Y. L. Park et al., "Design and control of a bio-inspired soft wearable robotic device for ankle-foot rehabilitation," *Bioinspiration and Biomimetics*, vol. 9, no. 1, p. 016007, 2014, Art. no. 016007.
- [3] L.-Q. Zhang et al., "Intelligent stretching of ankle joints with contracture spasticity," *IEEE Transactions on Neural Systems and Rehabilitation Engineering*, vol. 10, no. 3, pp. 149-157, September 2002.
- [4] P. K. Jamwal, S. Q. Xie, S. Hussain, and J. G. Parsons, "An adaptive wearable parallel robot for ankle injury treatments," *IEEE/ASME Transactions on Mechatronics*, vol. 19, no. 1, pp. 64-75, 2014.
- [5] Y. H. Tsoi, S. Q. Xie, and A. E. Graham, "Design, modeling and control of an ankle rehabilitation robot," *Studies in Computational Intelligence*, vol. 177, pp. 377-399, 2009.
- [6] J. A. Saglia, N. G. Tsagarakis, J. S. Dai, and D. G. Caldwell, "A high-performance redundantly actuated parallel mechanism for ankle rehabilitation," *The International Journal of Robotics Research*, vol. 28, no. 9, pp. 1216-1227, 2009.
- [7] M. Gironé, G. Burdea, M. Bouzit, V. Popescu, and J. E. Deutsch, "A Stewart platform-based system for ankle telerehabilitation," *Autonomous Robots*, vol. 10, no. 2, pp. 203-212, Mar 2001.
- [8] M. Zhang, T. C. Davies, and S. Xie, "Effectiveness of robot-assisted therapy on ankle rehabilitation - a systematic review," (in Eng), *Journal of NeuroEngineering and Rehabilitation*, vol. 10, p. 30, Mar 21 2013.
- [9] Y. N. Wu, M. Hwang, Y. P. Ren, D. Gaebler-Spira, and L. Q. Zhang, "Combined passive stretching and active movement rehabilitation of lower-limb impairments in children with cerebral palsy using a portable robot," *Neurorehabilitation and Neural Repair*, vol. 25, no. 4, pp. 378-385, May 2011.
- [10] G. Waldman et al., "Effects of robot-guided passive stretching and active movement training of ankle and mobility impairments in stroke," *NeuroRehabilitation*, vol. 32, no. 3, pp. 625-634, 2013.
- [11] J. E. Deutsch, J. A. Lewis, and G. Burdea, "Technical and patient performance using a virtual reality-integrated telerehabilitation system: preliminary finding," *IEEE Transactions on Neural Systems and Rehabilitation Engineering*, vol. 15, no. 1, pp. 30-35, March 2007.
- [12] J. A. Saglia, N. G. Tsagarakis, J. S. Dai, and D. G. Caldwell, "Control strategies for patient-assisted training using the ankle rehabilitation robot (ARBOT)," *IEEE/ASME Transactions on Mechatronics*, vol. 18, no. 6, pp. 1799-1808, 2013.
- [13] H. D. Taghirad and Y. B. Bedoustani, "An analytic-iterative redundancy resolution scheme for cable-driven redundant parallel manipulators," *IEEE Transactions on Robotics*, vol. 27, no. 6, pp. 1137-1143, 2011.
- [14] J. J. Craig, *Introduction to Robotics: Mechanics and Control*, 3rd ed. Prentice Hall, 2005.
- [15] M. Zhang, W. Meng, C. T. Davies, Y. Zhang, and S. Q. Xie, "A robot-driven computational model for estimating passive ankle torque with subject-specific adaptation," *IEEE Transactions on Biomedical Engineering*, vol. 63, no. 4, pp. 814 - 821, April 2016 2016.
- [16] R. Riener, L. Lünenburger, and G. Colombo, "Human-centered robotics applied to gait training and assessment," (in English), *Journal of Rehabilitation Research and Development*, vol. 43, no. 5, pp. 679-694, Aug/Sep 2006 2006.
- [17] H. Guo, Y. Liu, G. Liu, and H. Li, "Cascade control of a hydraulically driven 6-DOF parallel robot manipulator based on a sliding mode," *Control Engineering Practice*, vol. 16, no. 9, pp. 1055-1068, 2008.
- [18] K. McGehrin, A. Roy, R. Goodman, J. Rietschel, L. Forrester, and C. Bever, "Ankle robotics training in sub-acute stroke survivors: concurrent within-session changes in ankle motor control and brain electrical activity (P01.175)," *Neurology (P2 Neural Repair/Rehabilitation)*, vol. 78, no. 1\_MeetingAbstracts, 2012.
- [19] L. W. Forrester, A. Roy, H. I. Krebs, and R. F. Macko, "Ankle training with a robotic device improves hemiparetic gait after a stroke," *Neurorehabilitation and Neural Repair*, vol. 25, no. 4, pp. 369-377, May 2011.
- [20] A. Roy, L. W. Forrester, and R. F. Macko, "Short-term ankle motor performance with ankle robotics training in chronic hemiparetic stroke," *Journal of Rehabilitation Research and Development*, vol. 48, no. 4, pp. 417-430, 2011.
- [21] R. Lu, Z. Li, C. Y. Su, and A. Xue, "Development and Learning Control of a Human Limb With a Rehabilitation Exoskeleton," *IEEE Transactions on Industrial Electronics*, vol. 61, no. 7, pp. 3776-3785, 2014.
- [22] S. Hussain, S. Q. Xie, and P. K. Jamwal, "Adaptive impedance control of a robotic orthosis for gait rehabilitation," *IEEE Transactions on Cybernetics*, vol. 43, no. 3, pp. 1025-1034, 07 March 2013 2013.

- [23] P. K. Jamwal, S. Hussain, M. H. Ghayesh, and S. V. Rogozina, "Impedance Control of an Intrinsically Compliant Parallel Ankle Rehabilitation Robot," *IEEE Transactions on Industrial Electronics*, vol. 63, no. 6, pp. 3638-3647, 2016.
- [24] R. Riene and T. Edrich, "Identification of passive elastic joint moments in the lower extremities," *Journal of Biomechanics*, vol. 32, no. 5, pp. 539-544, 1999.
- [25] J. L. Emken, J. E. Bobrow, and D. J. Reinkensmeyer, "Robotic movement training as an optimization problem: designing a controller that assists only as needed," in *IEEE 9th International Conference on Rehabilitation Robotics*, Chicago, IL, USA, 2005: IEEE.
- [26] E. T. Wolbrecht, V. Chan, D. J. Reinkensmeyer, and J. E. Bobrow, "Optimizing compliant, model-based Robotic assistance to promote neurorehabilitation," *IEEE Transactions on Neural Systems and Rehabilitation Engineering*, vol. 16, no. 3, pp. 286-297, 2008.
- [27] S. K. Banala, S. H. Kim, S. K. Agrawal, and J. P. Scholz, "Robot assisted gait training with active Leg Exoskeleton (ALEX)," *IEEE Transactions on Neural Systems and Rehabilitation Engineering*, vol. 17, no. 1, pp. 2-8, Feb 2009.
- [28] R. Pérez-Rodríguez et al., "Anticipatory assistance-as-needed control algorithm for a multijoint upper limb robotic orthosis in physical neurorehabilitation," *Expert Systems with Applications*, vol. 41, no. 8, pp. 3922-3934, 2014.
- [29] J.-C. Metzger et al., "Assessment-driven selection and adaptation of exercise difficulty in robot-assisted therapy: a pilot study with a hand rehabilitation robot," *Journal of NeuroEngineering and Rehabilitation*, vol. 11, p. 154, 2014.
- [30] H. I. Krebs et al., "Rehabilitation robotics: performance-based progressive robot-assisted therapy," *Autonomous Robots*, vol. 15, no. 1, pp. 7-20, 2003.



Mingming Zhang received the M.Eng. degree in mechatronics from Chongqing University, China, in 2012, and the Ph.D. degree in mechanical engineering from the University of Auckland, Auckland, New Zealand, in 2016.

Since 2015, he has been working as a research assistant and/or visiting scholar in the Department of Mechanical Engineering at the University of Auckland. His research includes mechatronics, medical robotics, biomechanics, and advanced control techniques. He has

authored over 20 academic papers and 1 book. He also holds 6 patents.

Dr. Zhang has served as the invited reviewer for many high-quality international journals, including *IEEE Transactions on Mechatronics*, *IEEE Transactions on Biomedical Engineering*, and *IEEE Transactions on Industrial Electronics*. He is also the Executive Deputy Director of Auckland•Tongji Medical & Rehabilitation Research Center, Tongji Zhejiang College, China.



Sheng Q. Xie received the Ph.D. degrees from Huazhong University of Science and Technology, Wuhan, China, and the University of Canterbury, Christchurch, New Zealand, in 1998 and 2002, respectively.

From 2003 to 2016, he worked in the University of Auckland, New Zealand, where he chaired the research group of Biomechanics. Since 2017, he has joined the University of Leeds. He has published 5 books, 15 book

chapters, and more than 280 academic papers. His research interests include medical and rehabilitation robots and advanced robot control.

Prof. Xie was elected a Fellow of The Institution of Professional Engineers New Zealand in 2016. He has also served as a Technical Editor of the *IEEE/ASME Transactions on Mechatronics*.



Xiaolong Li received the Ph.D. degree in Management Science and Engineering from Southwest Jiaotong University, Chengdu, China, in 2003.

From 2003 and 2005, he worked in National maglev Engineering Technology Research Center (Shanghai of China) as a postdoctoral research fellow. He currently serves as a professor in Tongji University of China. He is the

author of 1 book and over 30 academic journal and conference papers. His research interests include rail transportation, mechatronics, and rehabilitation robotics.

Prof. Li is the Director of the Department of Science and Technology in Tongji Zhejiang College, China. He is also the Deputy Director of Auckland•Tongji Medical & Rehabilitation Research Center, Tongji Zhejiang College, China.



Guoli Zhu received the B.E. and M.E. degree in automation from Huazhong University of Science and Technology, Wuhan, China, in 1986 and 1989, respectively.

He currently serves as a professor with the School of Mechanical Science and Engineering at Huazhong University of Science and Technology. He is the author of 90 academic journal and conference papers, and 20 patents. His research interests include CNC machining, mechatronics, motion control, and rehabilitation robotics.



Wei Meng received the M.Eng. degree in information engineering from Wuhan University of Technology, Wuhan, China, in 2013. Since 2012, he has been a Doctoral Scholar working toward the joint Ph.D. degree in mechatronics engineering at Wuhan University of Technology and the University of Auckland, Auckland, New Zealand.

Since 2017, he has joined Wuhan University of Technology as a lecturer. He has over 25 academic journal and conference papers, and 2

patents. His research interests include robot-assisted rehabilitation, human-robot interaction, and iterative learning control.

Dr. Meng received the Best Paper Award at the 2016 International Conference on Innovative Design and Manufacturing. He is an Editor of *Cogent Engineering*.



Xiaolin Huang received the M.D. from Tongji Medical College in 1983, and the Ph.D. degree in Rehabilitation Science from Hong Kong Polytechnic University in 2000.

She is the Chair Professor of the Department of Rehabilitation Medicine at Tongji Hospital in Wuhan. Her research interests include neuro and musculoskeletal rehabilitation. She has published over 70 academic journal and

conference papers, and over 10 books.

Prof. Huang is currently the chief editor of *Chinese Journal of Physical Medicine and Rehabilitation* and *Chinese Journal of Rehabilitation Medicine*. She also serves as the vice president of Chinese Society of Rehabilitation Medicine, and the vice-director of Chinese Association of Physical Medicine and Rehabilitation.



Allan Veale received the B.E. degree in mechatronics engineering with first class honours from the University of Auckland, Auckland, New Zealand, in 2013.

Since 2013, he has been studying a Ph.D. degree in actuation technologies for wearable rehabilitation robots. During this research he published 3 journal articles and 2 conference papers. His research interests include the user-centered development of medical devices, fluidic muscle and dielectric elastomer actuators, soft sensor technologies, and novel portable energy sources.

soft sensor technologies, and novel portable energy sources.